Supplementary Figure 1

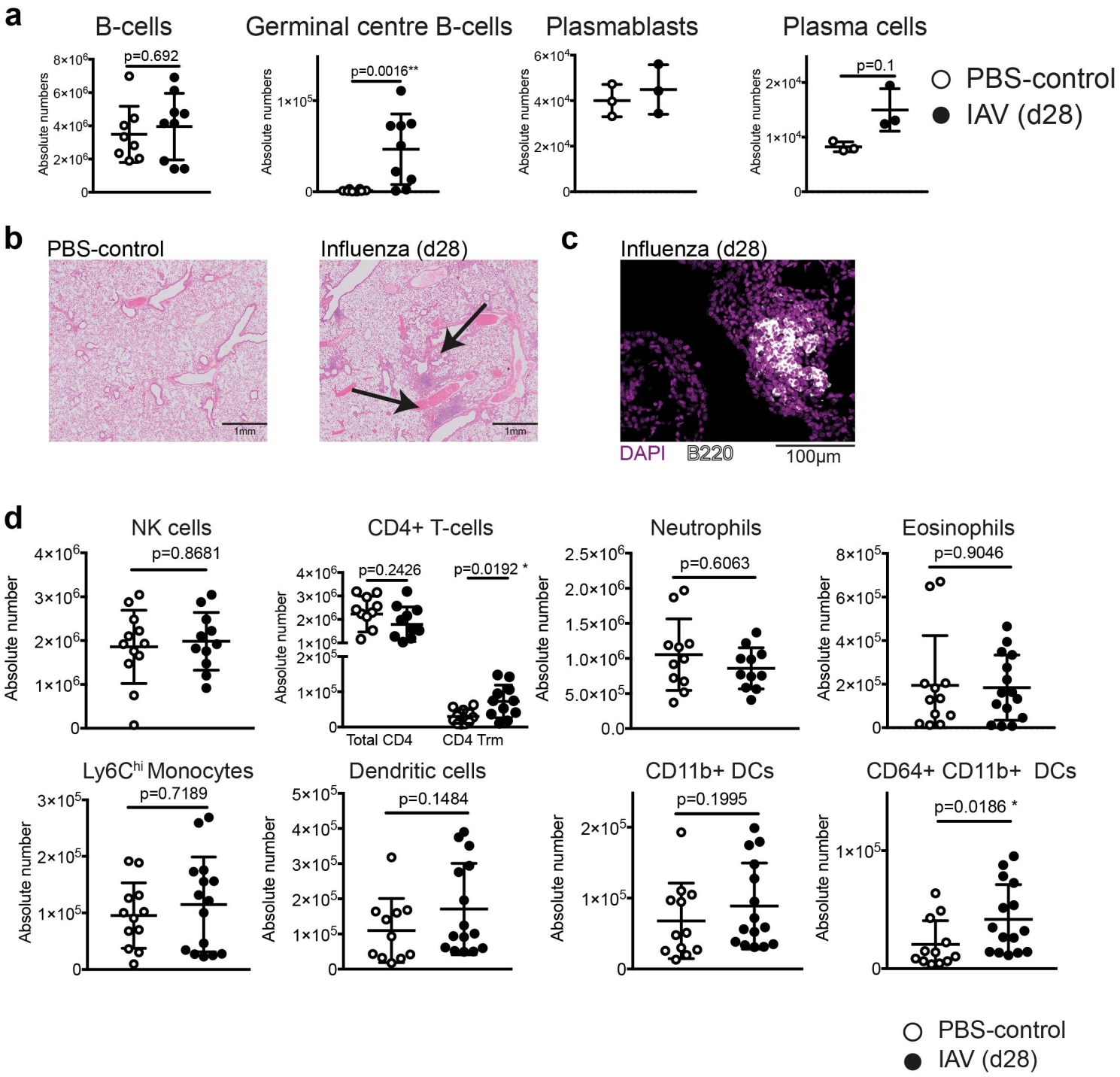

Supplementary figure 1: Immune cell composition in naïve and post-influenza mice.
a, Absolute number of total B-cells, and B-cell subsets in the lungs of naive and influenza experienced (IAV d28) mice, as quantified by flow cytometry. B-cells (n=8 mice PBS/n=9 mice X31), Plasma cells n=3 mice **b**, H&E staining of paraffin-embedded lung tissue sections from PBS-control and IAV d28 mice. **c**, B220/DAPI staining of a bronchial proximal follicle in a paraffin-embedded lung, 28 days post-influenza. Arrows indicate the presence of iBALT. **d**, Absolute number of innate and adaptive immune cell subsets in the whole lung of naive and influenza experienced (IAV d28) mice, as quantified by flow cytometry. CD4 T-cells (n=11 mice) Other cells (n=12 mice PBS/n=15 mice X31) from 3 independent experiments. Data shown as arithmetic means ±SD and statistical significance assessed using a two-tailed Mann Whitney U test. * p=≤0.05, ** p=≤0.01.

Supplementary Figure 2

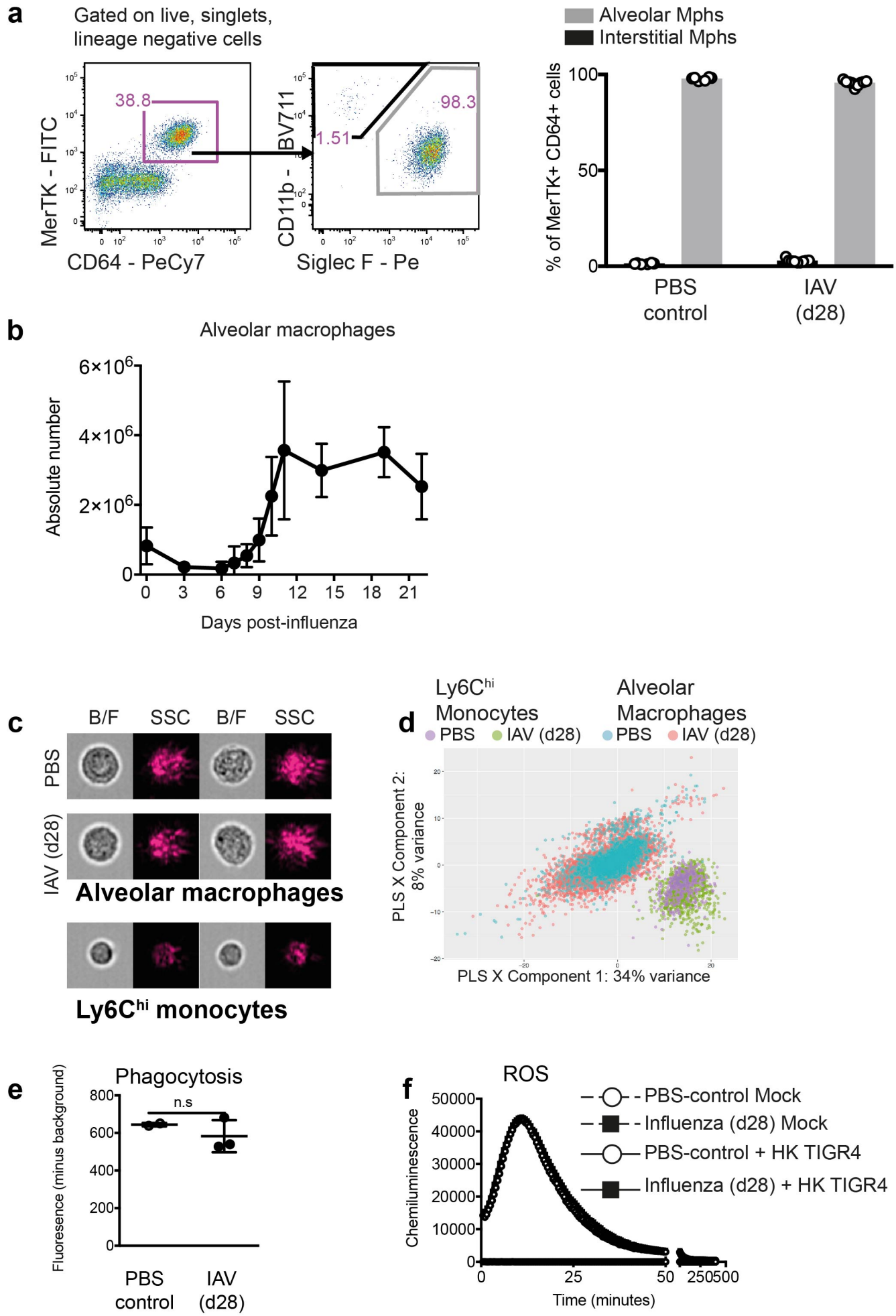

Supplementary figure 2: Characterisation of AM in naïve and post-influenza mice.

a, Alveolar macrophages ($CD64^+$ $MerTK^+$ $Siglec\ F^+$ $CD11b^-$) and interstitial macrophages ($CD64^+$ $MerTK^+$ $Siglec\ F^-$ $CD11b^+$) were quantified by flow cytometry in naïve and influenza-experienced lungs. **b**, Quantification of alveolar macrophages by flow cytometry in the lung at indicated time points following influenza infection. n=6 mice PBS/n=9 mice X31 from one experiment **c**, Imagestream of alveolar macrophages and $Ly6C^{hi}$ monocytes from naive and post-influenza lungs representative of 2 independent experiments. **d**, A partial least squares discriminant analysis (PLS-DA) of $Ly6C^{hi}$ monocytes and macrophages from naive and post-influenza lungs. **e**, Phagocytosis of live *S. pneumoniae* by alveolar macrophages. Bacteria were labelled with Carboxyfluorescein succinimidyl ester (CFSE) and incubated with AMs from naive (n=2 mice) and post-influenza (n=3 mice) lungs. Intracellular CFSE levels were quantified by flow cytometry. One representative experiment of two independent experiments is shown n.s. = 0.8 **f**, Reactive oxygen species (ROS) production by naïve (n=2 mice) and post-influenza (n=3 mice) alveolar macrophages. Chemiluminescence is detected by horseradish peroxidase reacting with cell-permeable luminol to detect both intracellular and extracellular ROS. Data shown as arithmetic means ±SD and statistical significance assessed by a two-tailed Mann Whitney Test.

Supplementary Figure 3

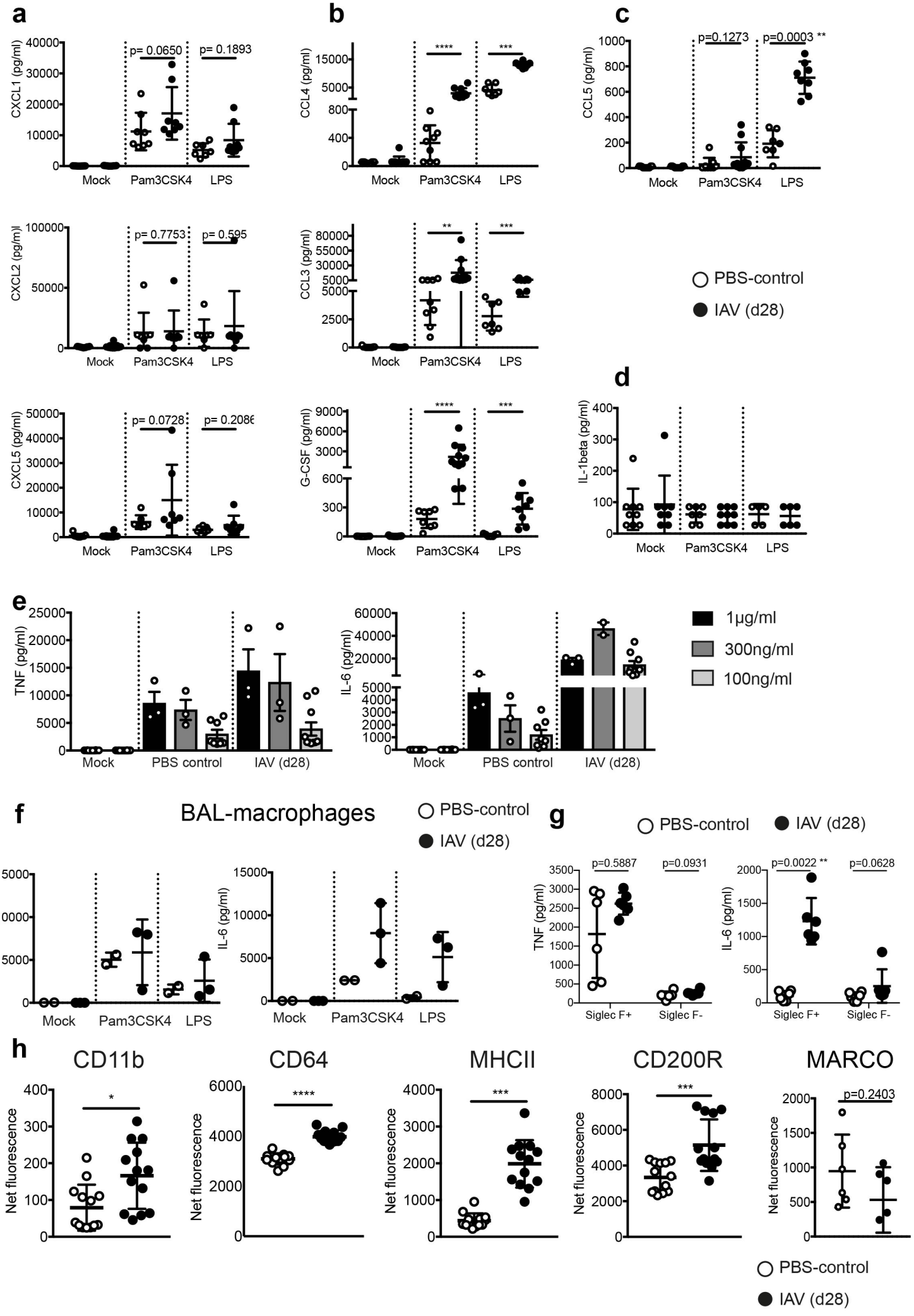

Supplementary Figure 3: Increased production of selective cytokines by post-influenza AMs.
a-d, Cytokine quantification by 36plex multiplex following a 16hr stimulation of AMs isolated from the lungs of naïve and influenza-experienced mice, stimulated *ex vivo* with 100ng/ml Pam3CSK4 or LPS. n= 9 mice (Pam3CSK4 PBS) n=8 mice (Pam3CSK4 IAV d28) n=7 mice (LPS PBS) n=8 mice (LPS IAV d28) from 2-3 independent experiments. **e**, Cytokine quantification of IL-6 and TNF by ELISA, from AMs isolated from the lungs of naïve and influenza-experienced mice, stimulated *ex vivo* with a range of Pam3CSK4 concentrations for 16 hours. **f,g**, Protein quantification of IL-6 and TNF by ELISA after *ex vivo* stimulation with 100ng/ml LPS (**f**) or Pam3CSK4 (**f,g**) for 16 hours, (**f**) from AMs isolated from BAL of naïve (n=2 mice) and influenza-experienced (n=3 mice) mice, or (**g**) from magnetically sorted SiglecF positive and negative cell fractions from the lungs of the indicated mice. (n=6 mice PBS/n=5 mice IAV d28) from one experiment. **h**, Expression of surface markers on alveolar macrophages quantified by flow cytometry n= 12 mice (PBS)/n=13 mice (X31) or (MARCO) n=6 mice (PBS)/n=5 mice (IAV d28) from 1-3 independent experiments. Net fluorescence indicates the subtraction of an FMO gMFI from the gMFI of the fluorophore. Data shown as arithmetic means ±SD and statistical significance assessed by two tailed Mann Whitney Test. * p=≤0.05, ** p=≤0.01, *** p=≤0.001, **** p=≤0.0001.

Supplementary Figure 4

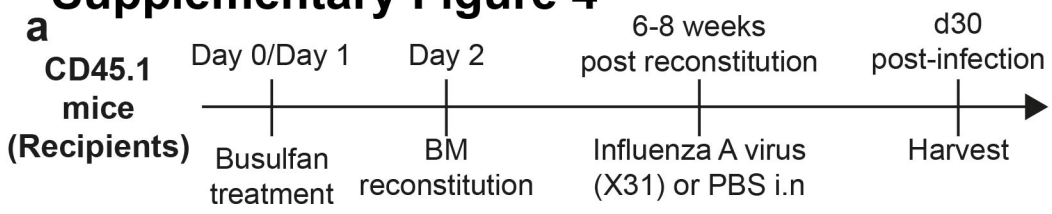

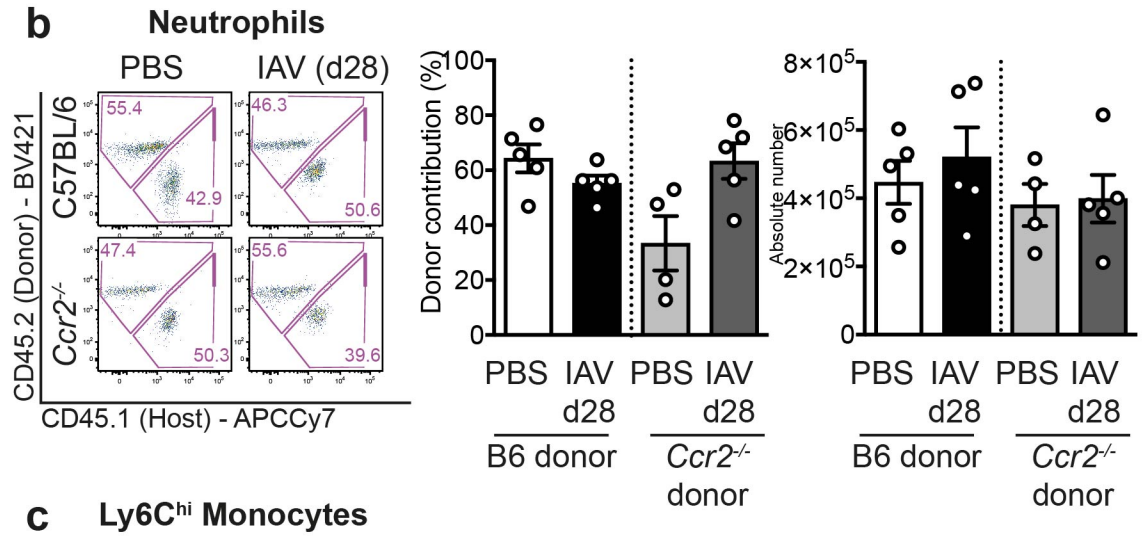

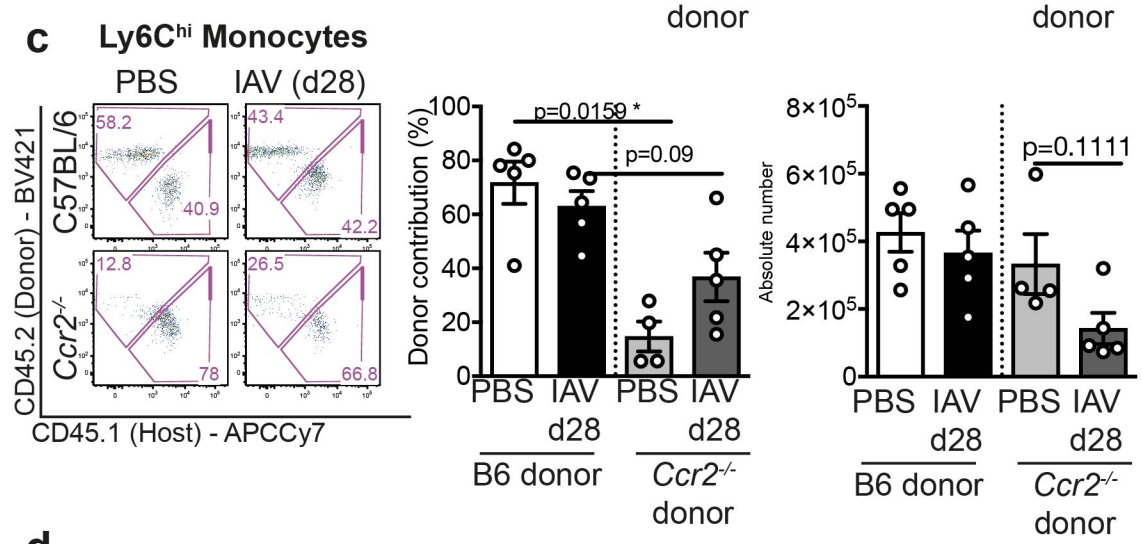

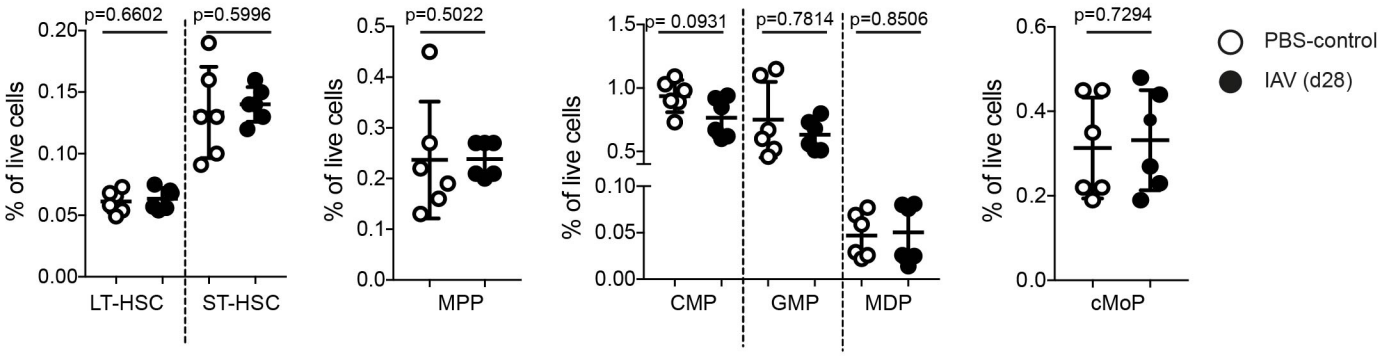

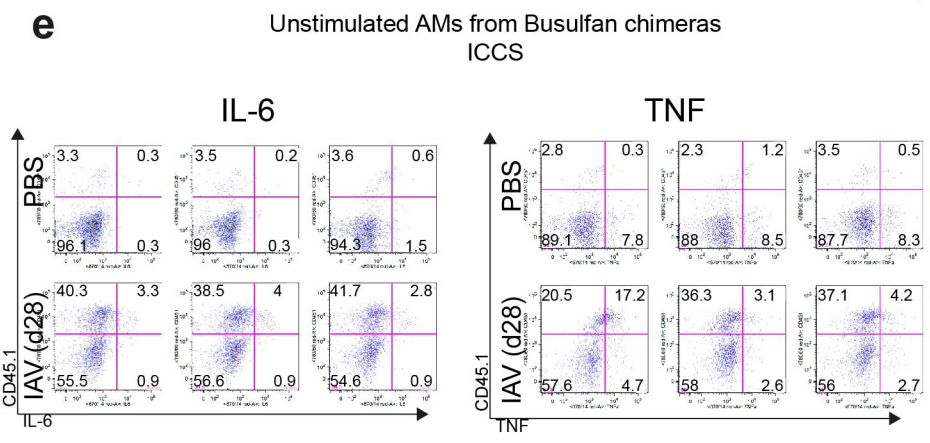

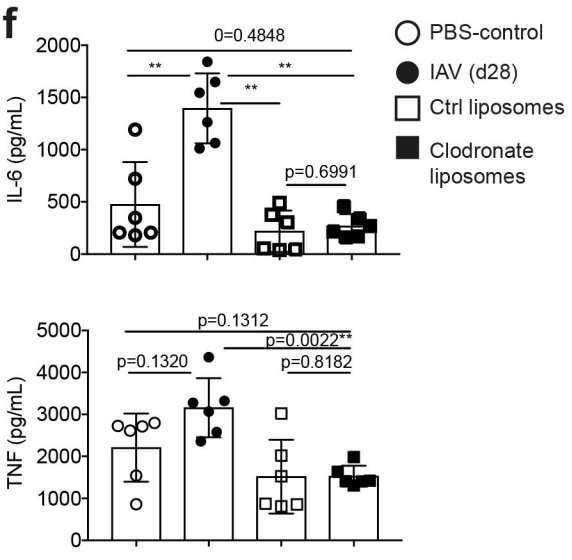

Supplementary Figure 4: Characterisation of Busulfan bone-marrow chimeras.

a, Schematic of Busulfan chimera experiments. **b,c,** Chimerism and absolute number of (**b**) neutrophils and (**c**) Ly6C^{hi} monocytes in the lungs of naïve (n=5 B6 donor/n=4 *Ccr2*$^{-/-}$ donor) and post-influenza (n=5 mice) Busulfan chimeras. From 2 independent experiments. **d**, Frequencies of myeloid progenitors in the bone marrow of naïve and influenza experienced (IAV d28) mice, identified as described in Methods. n=6 mice, pooled from 2 independent experiments. **e**, Naive and IAV (d28) alveolar macrophages were isolated from the lungs of chimeric mice and mock stimulated *ex vivo* to provide gating controls for **Fig 4e**. ICCS for IL6 (top panels) and TNF (bottom panels) n=4 mice **f**, C57BL/6 mice were treated with PBS (n=5), influenza (n=5 mice), PBS-liposomes (n=6 mice) or clodronate-liposomes (n=6 mice) as indicated. 28 days later, AMs were purified and stimulated in vitro with Pam3CSK4 for 16 hours. Cytokines were measured by ELISA. Pooled from 2 experiments. Data shown as arithmetic means ±SD and statistical significance assessed by two-tailed Mann Whitney Test. * p=≤0.05, ** p=≤0.01.

Supplementary Figure 5

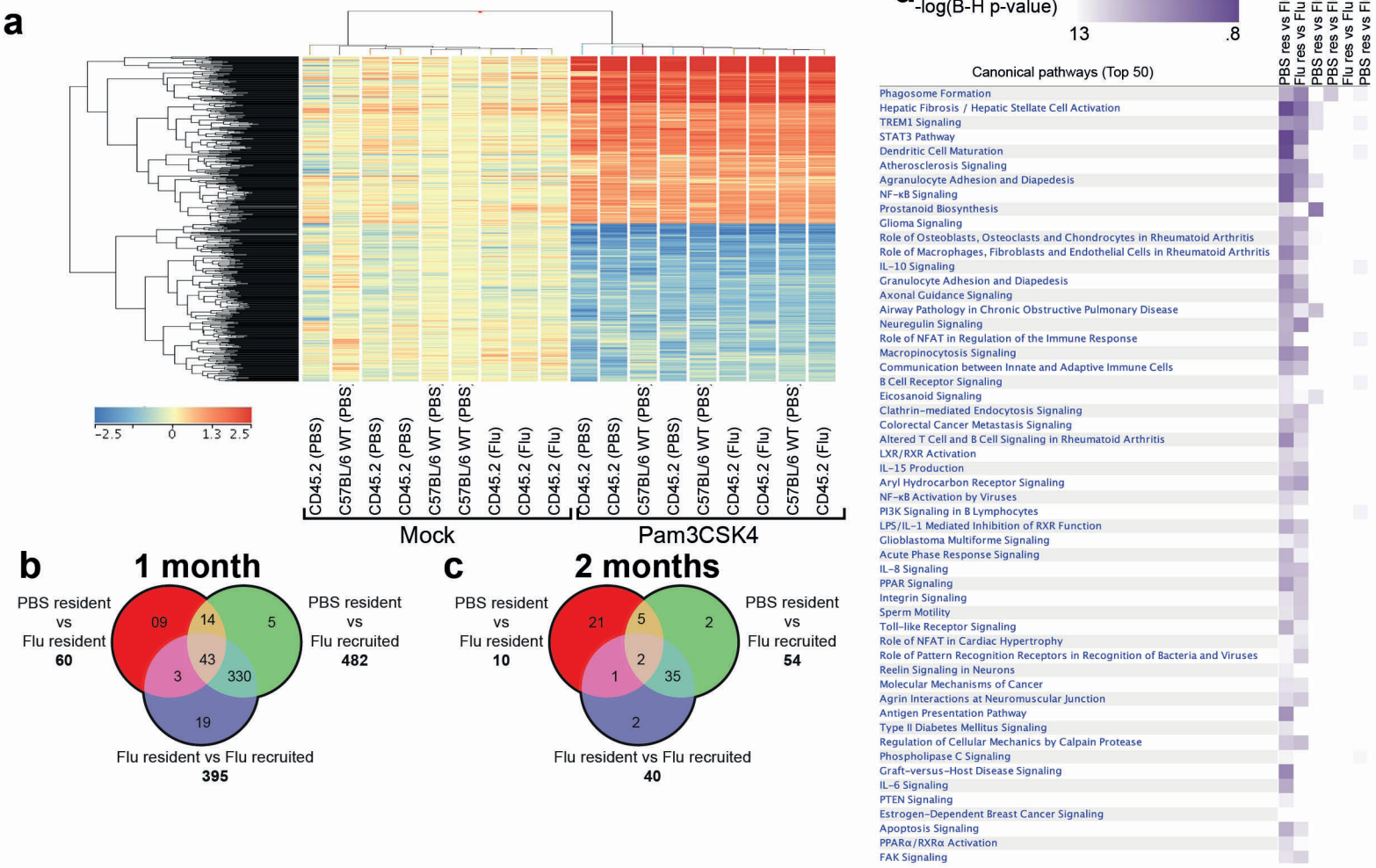

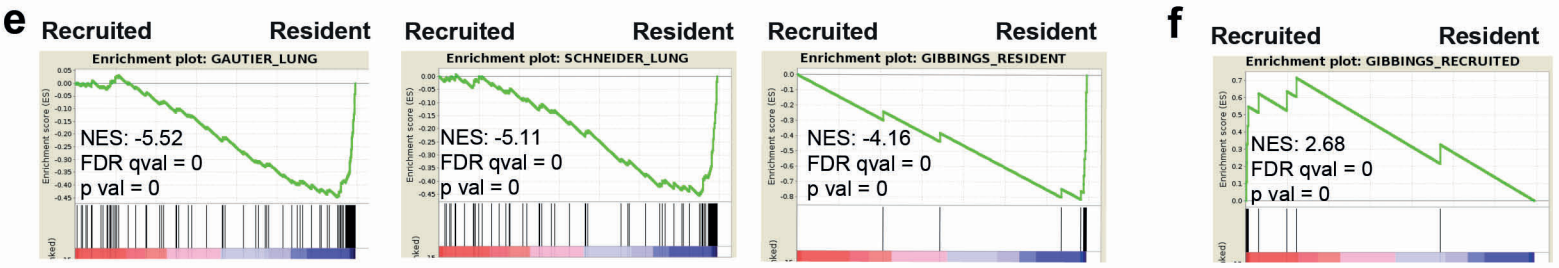

g

Influenza (d28): Recruited vs Resident

Name	NES	p-val
Cell cycle	3.89	0
E2F Pathway	3.74	0
Immune system	3.51	0
Cell cycle mitotic	3.44	0
PLK1 Pathway	3.27	0
Cell cycle	3.12	0

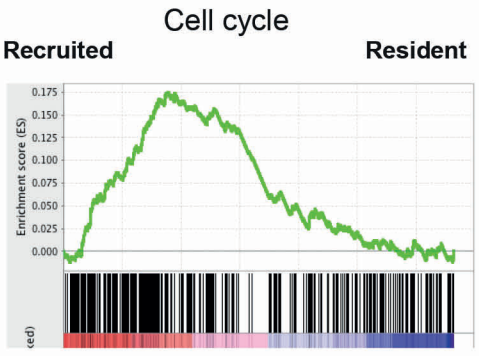

H2AFZ
CCNA2
RRM2
CDK1
CCNB1
PSMB9
CEP192
MCM6
NUMA1
CDC20

h

Influenza (d28): Recruited vs Resident

Name	NES	p-val
Metabolism of proteins	-4.57	0
Influenza life cycle	-4.19	0
Influenza Viral RNA transcription and replication	-4.17	0
3 UTR Mediated Translational Regulation	-4.1	0
KEGG Ribosome	-4.06	0

PABPC1
B4GALT6
MCFD2
GALNT1
FUT8
ST3GAL2
PROS1
PIGA
FBXL3
ARSB

Supplementary Figure 5: Transcriptome analysis of resident and recruited AMs from Busulfan chimeras at 1 month post-influenza.
a, Heat map of differentially expressed genes (FC>2, 2-way ANOVA with Benjamini-Hochberg correction, p<0.01). Variables are stimulation (Mock, Pam3CSK4) and origin (CD45.2 PBS, CD45.2 Flu: resident AMs from Busulfan chimeras and therefore of a *Ccr2*$^{-/-}$ genotype; and C57BL/6 WT PBS: resident AMs from naïve C57BL/6 mice and therefore of a CCR2wt genotype). Unsupervised clustering for treatment groups shows great similarity of *Ccr2*$^{-/-}$ and WT resident AMs. **b,c**, Venn diagram showing the pairwise comparisons between mock-stimulated samples at 1 month (**b**) or 2 months (**c**) post-influenza. **d**, Heatmap for significant differences in Canonical pathways for the 6 pairwise comparisons shown in (**b**) and (**c**). Gene expression was compared using IPA Comparison Analysis. **e,f**, GSEA using published gene sets derived from Gautier et al.[29], Gibbings et al.[17], Lavin et al.[30], Schneider et al.[31] depicting gene sets which are enriched in resident AMs (e) or in recruited AMs (**f**) at 28 days post influenza. **g,h**, Top 5 pathways (FDR q-val <0.01) found by GSEA to be enriched in recruited (**g**) or resident (**h**) alveolar macrophages (NES = Normalized Enrichment Score). Included are representative GSEA plots from and the top 10 highest ranked genes from the indicated gene set.

Supplementary Figure 6

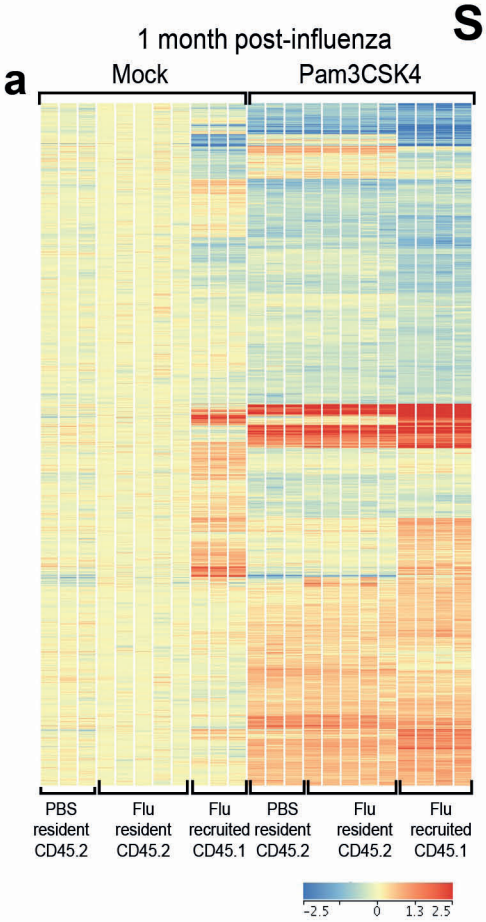

b Top 5 pathways GREAT analysis

	Pathway name	Binom Raw p-Value	Binom FDR Q-Value
Cluster 1	Immune system process	5.15E-182	5.76E-179
	Regulation of immune system process	5.33E-123	1.85E-120
	Leukocyte activation	1.61E-122	4.16E-110
	Positive regulation of immune system process	1.52E-105	3.34E-103
	Immune system development	1.00E-103	1.99E-101
Cluster 2	Regulation of cell cycle	5.30E-62	8.91E-59
	Positive regulation of epithelial to mesenchymal transition	1.60E-27	3.23E-25
	Regulation of epithelial to mesenchymal transition	2.01E-27	3.99E-25
	Fatty acid metabolic process	2.86E-24	4.00E-22
	Negative regulation of epithelial cell proliferation	3.59E-24	4.83E-22
Cluster 3	Immune system process	0.00E+00	0.00E+00
	Regulation of immune system process	4.73E-239	1.59E-235
	Immune response	5.45E-229	1.37E-225
	Response to other organism	1.73E-216	3.49E-213
	Defense response	6.60E-210	9.49E-207
Cluster 4	Lipid storage	2.85E-31	3.49E-29
	Vacuole organization	1.31E-30	1.54E-28
	Regulation of gene expression, epigenetic	7.08E-29	7.50E-27
	Gene silencing	1.55E-19	8.33E-18
	DNA methylation or demethylation	1.61E-19	8.59E-18

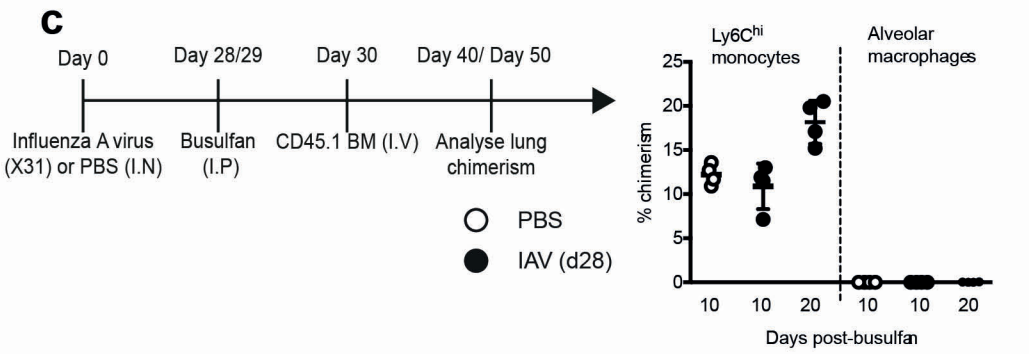

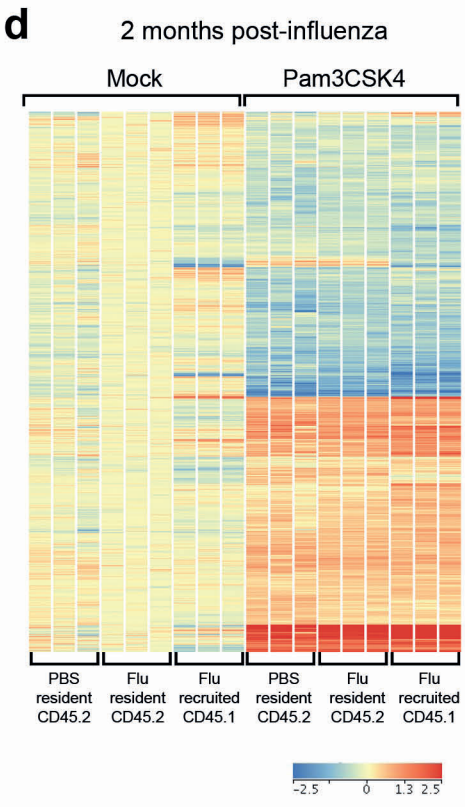

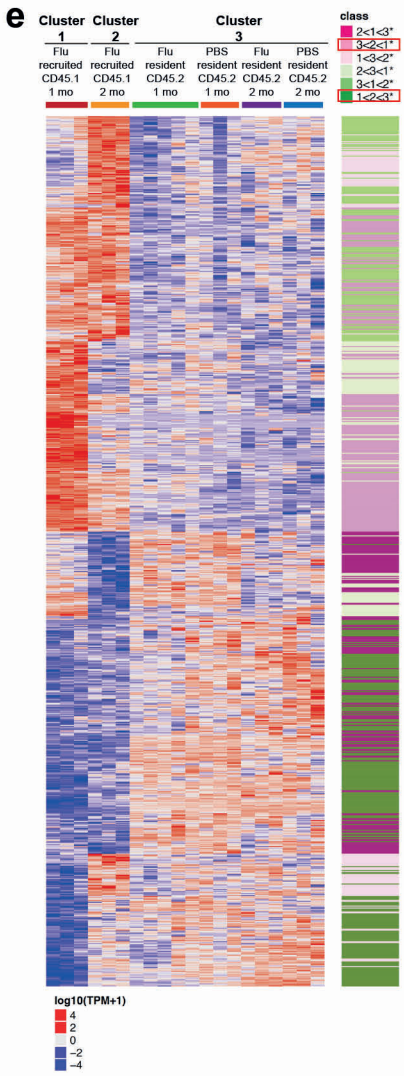

Supplementary Figure 6: Transcriptome analysis of resident and recruited AMs from Busulfan chimeras at 2 months post-influenza.
a,d, Heatmap of differentially expressed genes at 1 month (**a**) or 2 months (**d**) post infection (FC>1.5, 2-way ANOVA with Benjamini-Hochberg correction, p<0.01). Variables are stimulation (Mock, Pam3CSK4) and origin (CD45.2 (*Ccr2*$^{-/-}$) PBS resident, CD45.2 (*Ccr2*$^{-/-}$) Flu resident, CD45.1 Flu recruited). **b**, The p-values and FDR q-values of the Top 5 GO Biological processes enriched in genes annotated by GREAT to each cluster in Fig. 6e. **c**, Schematic of infection and Busulfan treatment to identify influx of BM-derived monocytes after influenza resolution. Chimerism was identified by CD45.1 positive cells in Ly6C^{hi} monocytes and alveolar macrophages in the lung at 10 and 20 days post-reconstitution. **e**, Genes from unstimulated cells at one and two months post influenza as shown in **Fig. 7g** were grouped into the three clusters indicated. Genes were then classified by their changes between clusters into the six classes indicated. Two of these classes (increasing expression over time of lung residence, cluster1<2<3; and decreasing expression over time of lung residence, cluster3<2<1) were further analysed. **f**, GSEA for the two classes defined in (**e**).

Supplementary Figure 7

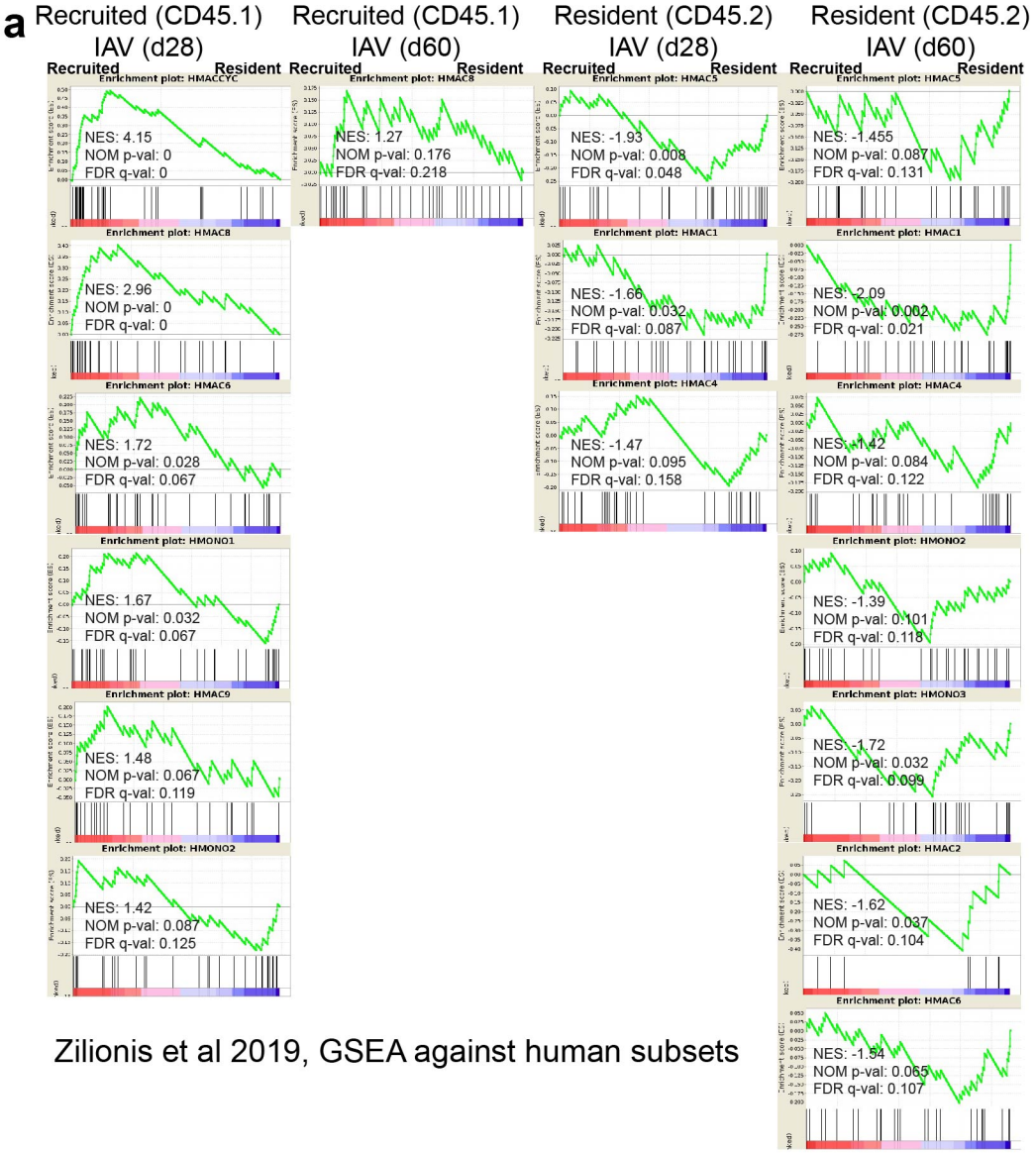

Zilionis et al 2019, GSEA against human subsets

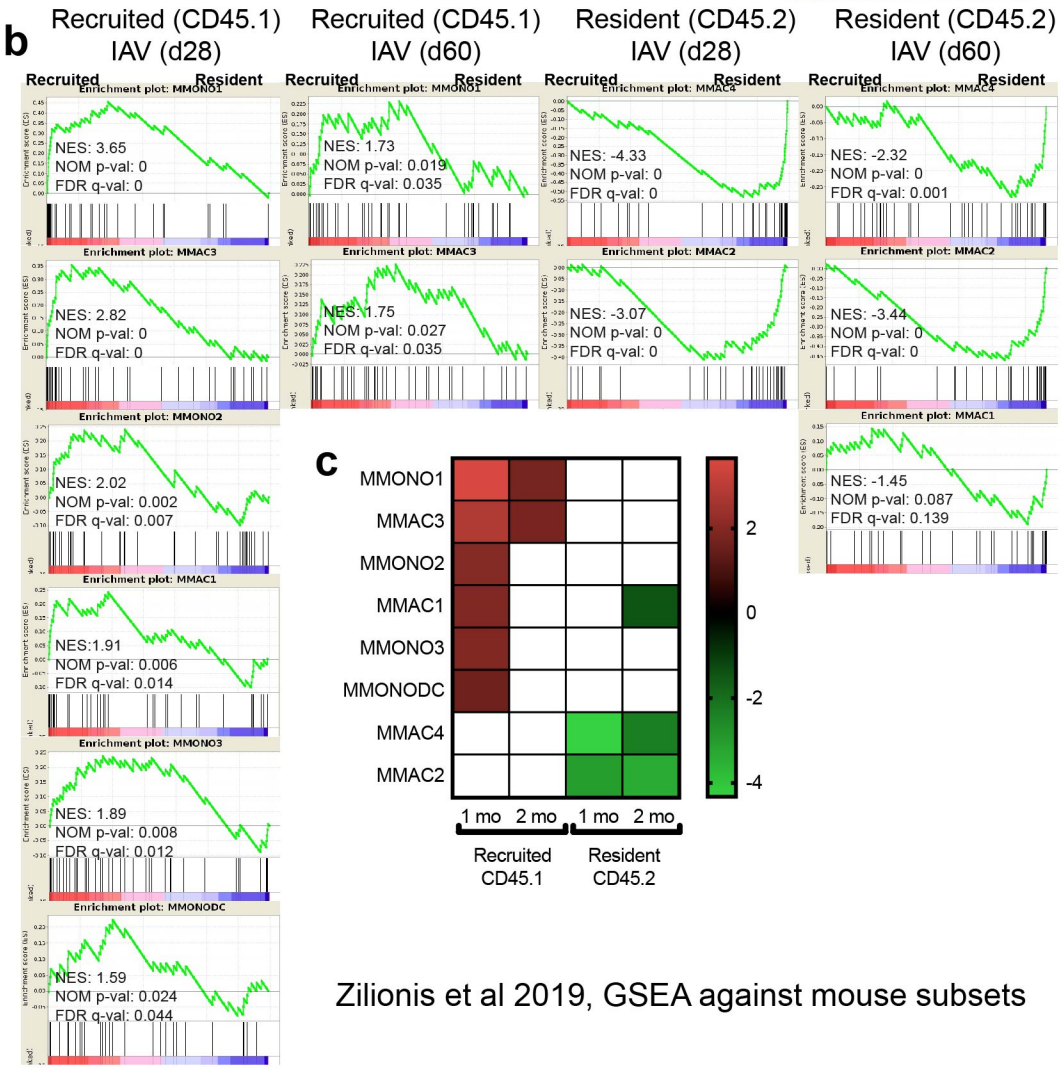

Zilionis et al 2019, GSEA against mouse subsets

Supplementary Figure 7: Comparison between resident and recruited AMs to human and mouse lung macrophage gene sets in lung cancer.
GSEA using a ranked gene list of recruited versus resident AMs at one or two month post influenza, (**a**) human and (**b**) mouse gene sets from lung macrophages, monocytes and dendritic cells obtained from Zilionis et al.[34]. **c**, Heatmap showing the NES of GSEA performed using mouse datasets obtained from Zilionis et al.[34].

Supplementary Figure 8

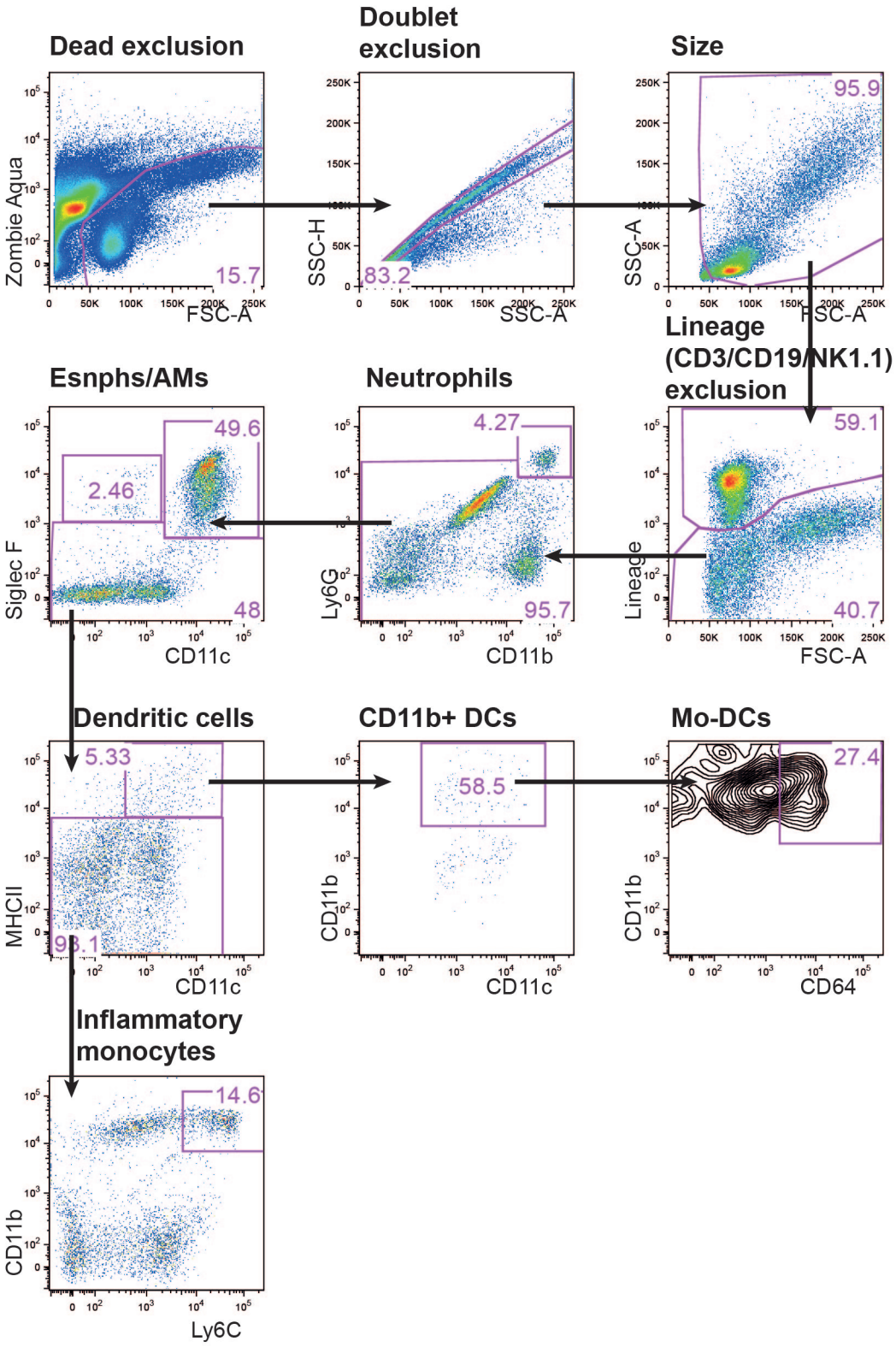

Supplementary figure 8: Myeloid gating strategy for whole lung
Gating strategy, exemplified in an influenza (d28) lung

Supplementary Figure 8: Flow-based identification of myeloid cells in the lung.
Gating strategy for myeloid cells in the lung, exemplified in an IAV (d28) lung.